

An Effective TiO₂ Photocatalyst Prepared under Supercritical Conditions

Hexing Li,* Jian Zhu, Guisheng Li, and Ying Wan

Department of Chemistry, Shanghai Normal University, Shanghai 200234, P. R. China

(Received February 2, 2004; CL-040126)

A novel porous TiO₂ photocatalyst with higher surface area was prepared by sol-gel method followed by removing solvent under supercritical conditions. This catalyst exhibited higher activity and stronger durability during photocatalytic degradation of phenol than that obtained via direct drying, possibly owing to the higher surface area and crystallization degree of anatase which exhibited higher quantum yield during photocatalysis.

Recently, photocatalysis has caused much attention owing to its wide application in complete mineralization of various organic pollutants in waste water and air. Among various photocatalysts, TiO₂ is most frequently employed owing to its cheapness, nontoxicity, and structural stability.¹⁻³ However, TiO₂ semiconductors could be activated only by UV light because of its high energy band gap. Besides, the low quantum efficiency of the TiO₂ seems also a problem limiting its application. Up to now, many attempts have been made to improve the catalytic performance of the TiO₂, such as modification with metallic ions or other oxides.⁴ On the other hand, very little attention has been paid to development of new preparation method. Sol-gel is probably the most frequently employed method for preparing TiO₂. The solvent in the gel (TiO₂ precursor) was usually removed by direct drying, followed by calcination. However, the direct drying of the TiO₂ gel might cause the gathering of the small particles and more severely, the collapse of the pore structure. Many studies have confirmed that treatment of the catalyst precursor under supercritical conditions might preserve its pore structure as that in the gel after the solvent was removed.⁵ We reported here a porous TiO₂ nanoparticles prepared by sol-gel method followed by drying the precursor under supercritical conditions to remove solvent. During liquid-phase photocatalytic degradation of phenol, the as-prepared TiO₂ catalyst exhibited much higher activity than that obtained via direct drying. The correlation of the photocatalytic properties to structural and photoluminescent characteristics was discussed briefly.

The TiO₂ nanoparticles were prepared by the following procedure: At 313 K, 2.5-mL dilute HNO₃ solution (1:5 V/V) was added dropwise into 50-mL solution containing 10 mL Ti(*n*-OC₄H₉)₄ and 40 mL alcohol (EtOH) under vigorous stirring. After stirring for 3 h, the TiO₂ sol was aged at 313 K for another 72 h. The resulting TiO₂ xerogel was transferred into to a 500-mL autoclave containing 250 mL EtOH. Then, the autoclave was heated at the rate of 4 K/min until 533 K, at which the pressure may reach 8.0 MPa. The system was kept at that temperature and pressure for 2 h and then the alcohol vapor was excluded slowly from the autoclave until the inside pressure decreased down to atmospheric pressure. After being cooled down to room temperature in N₂ flow, the TiO₂ nanoparticles were obtained, which were further calcined for 12 h at a given temperature. The TiO₂ obtained in that way was marked as SC. For comparison, the direct drying method was also used to remove solvent in the TiO₂ gel and the resulting TiO₂ sample was marked as DC.

The structure of the as-prepared TiO₂ samples was determined by X-ray diffraction (XRD, Rigacu D' max-3C). As shown in

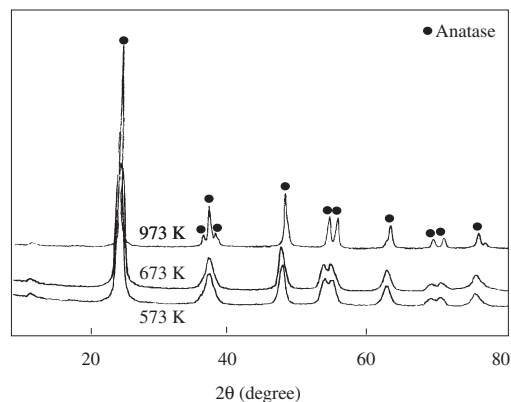


Figure 1. XRD patterns of the TiO₂ (SC) calcined at different temperatures.

Figure 1, the TiO₂ (SC) sample exhibited well-crystallized anatase phase. Calcination of the TiO₂ (SC) sample at elevated temperature from 573 to 973 K resulted in a slight enhancement of the crystallization degree of the anatase phase. No significant rutile phase appeared even at 973 K, showing the excellent thermal stability of the TiO₂ (SC). Unlike the TiO₂ (SC), the TiO₂ (DC) was present in amorphous state after being calcined at 573 K since only one broad peak around $2\theta = 25^\circ$ was observed on the XRD pattern. Even at 673 K, the crystallization degree was still very poor. Treatment at 973 K resulted in well-crystallized anatase phase, but such treatment also caused a structural transformation from anatase to rutile phase owing to the poor thermal stability. On the basis of the transmission electron micrograph (TEM, JEM-2010), it was found that both the TiO₂ (SC) and TiO₂ (DC) samples were present in the spherical nanoparticles with the similar particle size around 10–20 nm. However, the nanoparticles in the TiO₂ (SC) distributed more homogeneously than those in the TiO₂ (DC). After being treated at 973 K, large particles and even big lumps were observed because of the gathering of small particles at high temperature. From the isothermal curves of nitrogen adsorption and desorption at 77 K, one can see that both the TiO₂ (SC) and TiO₂ (DC) exhibited porous structure. Their surface area (S_{BET}), pore volume (V_{P}) and average pore diameter (d_{p}) were calculated by using BJH method. These structural parameters were summarized in Table 1.

As shown in Table 1, the TiO₂ (SC) exhibited much higher surface area than the TiO₂ (DC) when they were calcined at the same temperature. As mentioned above, the TEM morphologies demonstrated that both the samples exhibited similar particle size. Thus, one could conclude that the higher surface area of the TiO₂ (SC) was mainly attributed to its larger pore volume and pore size. This could be easily understood by considering the unique role of the supercritical conditions since removing solvent under such conditions might maintain the pore structure as that in the gel owing to the lack of surface-tension effect, whereas severe collapse of the pore structure would occur when the solvent in the gel was removed by direct drying. When the calcination temperature increased from 573 to 673 K, both the pore volume and surface area in-

Table 1. Structural and catalytic property of the TiO₂ samples^a

Catalyst	T _{calcination} /K	V _p /cm ³ /g	d _p /nm	S _{BET} /m ² /g	Degradation Yield
TiO ₂ (DC)	573	0.029	5.3	22	38%
	673	0.037	5.4	27	50%
	973	0.001	–	10	18%
TiO ₂ (SC)	573	0.45	19	78	70%
	673	0.46	20	81	78%
	973	0.15	21	28	64%
TiO ₂ (P25)	as-received	0.25	20	45	95%

^aReaction conditions: 0.05 g catalyst, 30 mL of 1.0 mmol/L phenol aqueous solution, T = 301 K, 8-W mercury lamp (mixture of 254, 310, and 365 nm) as light source, stirring rate = 1000 rpm, reaction time = 4 h.

creased slightly, possibly owing to the removal of residual organic impurity in the pore channel and on the surface, as confirmed by IR spectra. Further increase in the calcination temperature caused a severe collapse of the pore structure and gathering, resulting in an abrupt decrease in pore volume and thus, in surface area. Generally, the influence of calcination temperature on the TiO₂ (SC) was much less than that on the TiO₂ (DC), indicating that the former possessed better thermal stability.

The photocatalytic degradation of phenol was carried out at 301 ± 0.2 K in a 100-mL beaker containing 0.05 g catalyst, 30 mL of 1.0 mmol/L phenol aqueous solution. The reaction suspension was stirred for 1 h until the adsorption equilibrium was achieved. Then, a 8-W high-pressure mercury lamp comprised of 254, 310, and 365 nm mixed UV lights were applied at 2 cm above the reaction system to initiate the photocatalysis. During the reaction, the stirring rate was controlled at 1000 rpm that was high enough to eliminate the diffusion effect. After reaction for 4 h, the catalyst was separated from the solution and the phenol left in the solution was analyzed by a UV spectrophotometer (UV 7504/PC) at λ = 270 nm, from which the phenol degradation yield (%) was calculated by comparing the initial content of phenol in the solution. According to product analysis by HPLC (25 × 0.46 cm SPHERISORB ODS column, 50% methanol–water mobile phase, UV detector), only the phenol was identified, showing the complete decomposition of phenol to carbon dioxide during the present photocatalysis. The reference experiment revealed that, after reaction for 4 h under the same conditions, the phenol degradation in the absence of either the catalyst or the UV light was less than 5% and thus, could be neglected in comparison with that in the presence of both the catalyst and UV source. The reproducibility of the results was checked by repeating the runs at least three times and was found to be within acceptable limits (±5%).

The degradation yields of phenol over various TiO₂ photocatalysts were summarized in Table 1. For both the TiO₂ (DC) and TiO₂ (SC) photocatalysts, their activities first increased and then decreased with the increase of calcination temperature from 573 to 973 K. The optimum calcination temperature was determined as 673 K. When the calcination temperature increased from 573 to 673 K, the activity increased slightly, possibly owing to the increase of both the surface area and the crystallization degree of the anatase phase.⁶ Further increase in the calcination temperature to 973 K resulted in an abrupt decrease in the activity of TiO₂ (DC) because of the abrupt decrease in the surface area and especially, the structural transformation from anatase to rutile phase, which was less active.⁷ Although an abrupt decrease in the surface area of the TiO₂ (SC) was also observed after being treated at 973 K, its activity decreased by only 18% since no rutile phase appeared. In comparison with the TiO₂ (DC) treated at the same conditions, the TiO₂ (SC) exhibited much higher activity. Besides, the TiO₂ (SC) also exhibited much longer lifetime than the TiO₂ (DC) since the TiO₂ (SC) could be used repetitively for more than 8 times

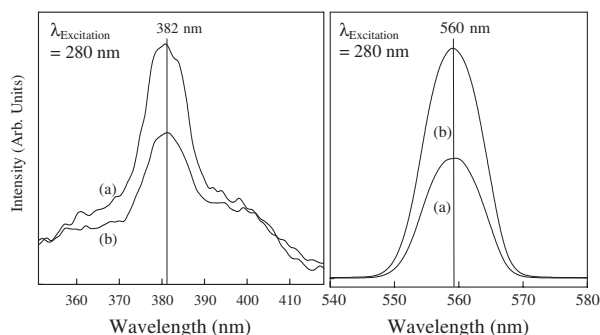


Figure 2. PL spectra of (a) the TiO₂ (SC) and (b) the TiO₂ (DC) after being calcined at 673 K. The excited wavelength was 280 nm.

(32 h) without significant decrease in the activity while the activity of the TiO₂ (DC) decreased by more than 20% even after being used repetitively for 3 times (12 h). One possible reason accounting for the higher activity of the TiO₂ (SC) was its higher surface area. However, the more important factor was the higher crystallization degree of the TiO₂ (SC) which was confirmed by the fact that the TiO₂ (SC) treated at 973 K still exhibited much higher activity than the TiO₂ (DC) treated at 673 K though both the samples had the similar surface area. In order to elucidate the promoting effect of the crystallization degree on the photocatalytic activity, the photoluminescent (PL) spectra were recorded on a Varian Cary-Eclipse 500. As shown in Figure 2, both the TiO₂ samples exhibited two PL peaks. The signal at about 382 nm could be attributed to emission-signal peak from band edge free excitation, mainly corresponding to the oxygen vacancies or other defects of the TiO₂ particles.⁸ While, the signal at about 560 nm was assigned to be the dual-frequency peak, indicative of the adsorption of UV light by the TiO₂ particles.⁷ The TiO₂ (SC) exhibited stronger emission peak at 382 nm, implying the presence of more oxygen vacancies or other defects which could capture the photoinduced electrons and thus, could effectively inhibit the recombination of the photoinduced electrons and holes. Meanwhile, the weaker emission peak at 560 nm demonstrated that the TiO₂ (SC) may absorb more UV light which might generate more charge carriers served as active sites for phenol degradation. Thus, the TiO₂ (SC) exhibited higher quantum yield than the TiO₂ (DC). Although the TiO₂ (SC) exhibited higher activity than TiO₂ (DC), its activity was still lower than the commercially available P25, as shown in Table 1. Since the P25 exhibited lower pore volume and surface area than the TiO₂ (SC) but their pore sizes were almost the same, one may conclude that other factors, such as the particle size, the distribution of pore size, the ratio between anatase and rutile etc., also played important roles in determining the activity. Detailed studies are being underway.

This work was supported by the National Natural Science Foundation of China (20377031) and the Natural Science Foundation of Shanghai (03DJ14005).

References

- 1 A. Fujishima, T. N. Rao, and D. A. Tryk, *J. Photochem. Photobiol., C*, **1**, 1 (2000).
- 2 J. M. Hermann, C. Guillard, J. Disdier, C. Lehaut, S. Maltao, and J. Blanco, *Appl. Catal., B*, **35**, 281 (2002).
- 3 D. W. Bahnemann, S. N. Kholuisakaya, R. Dillert, A. I. Kulak, and A. Kokorin, *Appl. Catal., B*, **36**, 161 (2002).
- 4 E. Piera, J. A. Ayllon, X. Domenech, and J. Peral, *Catal. Today*, **76**, 259 (2002).
- 5 J. F. Bocquet, K. Chhor, and C. Pommier, *Mater. Chem. Phys.*, **57**, 274 (1999).
- 6 S. Yamazaki, N. Fujinaga, and K. Araki, *Appl. Catal., A*, **210**, 97 (2003).
- 7 A. L. Linsebigler, G. Lu, and J. T. Yates, Jr., *Chem. Rev.*, **95**, 735 (1995).
- 8 L. D. Zhang and C. M. Mou, *Nanostruct. Mater.*, **6**, 831 (1995).